Proposed Inclusive Dark Photon Search at LHCb

Philip Ilten,[1,*] Yotam Soreq,[2,†] Jesse Thaler,[2,‡] Mike Williams,[1,§] and Wei Xue[2,‖]

[1]*Laboratory for Nuclear Science, Massachusetts Institute of Technology, Cambridge, Massachusetts 02139, USA*
[2]*Center for Theoretical Physics, Massachusetts Institute of Technology, Cambridge, Massachusetts 02139, USA*
(Received 7 April 2016; published 23 June 2016)

We propose an inclusive search for dark photons A' at the LHCb experiment based on both prompt and displaced dimuon resonances. Because the couplings of the dark photon are inherited from the photon via kinetic mixing, the dark photon $A' \to \mu^+\mu^-$ rate can be directly inferred from the off-shell photon $\gamma^* \to \mu^+\mu^-$ rate, making this a fully data-driven search. For run 3 of the LHC, we estimate that LHCb will have sensitivity to large regions of the unexplored dark-photon parameter space, especially in the 210–520 MeV and 10–40 GeV mass ranges. This search leverages the excellent invariant-mass and vertex resolution of LHCb, along with its unique particle-identification and real-time data-analysis capabilities.

Dark matter—firmly established through its interactions with gravity—remains an enigma. Though there are increasingly stringent constraints on direct couplings between visible matter and dark matter, little is known about the dynamics within the dark sector itself. An intriguing possibility is that dark matter might interact via a new dark force, felt only feebly by standard model (SM) particles. This has motivated a worldwide effort to search for dark forces and other portals between the visible and dark sectors (see Ref. [1] for a review).

A particularly compelling dark-force scenario is that of a dark photon A' which has small SM couplings via kinetic mixing with the ordinary photon through the operator $(\epsilon/2)F'_{\mu\nu}F^{\mu\nu}$ [2–7]. Previous beam dump [7–21], fixed target [22–24], collider [25–27], and rare meson decay [28–37] experiments have already played a crucial role in constraining the dark photon mass $m_{A'}$ and kinetic-mixing strength ϵ^2. Large regions of the $m_{A'} - \epsilon^2$ plane, however, are still unexplored (see Fig. 1). Looking to the future, a wide variety of innovative experiments have been proposed to further probe the dark photon parameter space [38–48], though new ideas are needed to test $m_{A'} > 2m_\mu$ and $\epsilon^2 \in [10^{-7}, 10^{-11}]$.

In this Letter, we propose a search for dark photons via the decay

$$A' \to \mu^+\mu^-, \tag{1}$$

at the LHCb experiment during LHC run 3 (scheduled for 2021–2023). The potential of LHCb to discover dark photons was recently emphasized in Ref. [48], which exploits the exclusive charm decay mode $D^* \to D^0 A'$ with $A' \to e^+e^-$. Here, we consider an inclusive approach where the production mode of A' need not be specified. An important feature of this search is that it can be made fully data driven, since the A' signal rate can be inferred from measurements of the SM prompt $\mu^+\mu^-$ spectrum. The excellent invariant-mass and vertex resolution of the LHCb detector, along with its unique particle-identification and real-time data-analysis capabilities [50,51], make it highly sensitive to $A' \to \mu^+\mu^-$. We derive the LHCb sensitivity for both prompt and displaced A' decays, and show that LHCb can probe otherwise inaccessible regions of the $m_{A'} - \epsilon^2$ plane.

The A' is a hypothetical massive spin-1 particle that, after electroweak symmetry breaking and diagonalizing the gauge kinetic terms, has a suppressed coupling to the electromagnetic (EM) current J_{EM}^μ [2–7]:

$$\mathcal{L}_{\gamma A'} \supset -\frac{1}{4}F'_{\mu\nu}F'^{\mu\nu} + \frac{1}{2}m_{A'}^2 A'^\mu A'_\mu + \epsilon e A'_\mu J_{EM}^\mu. \tag{2}$$

There is also a model-dependent coupling to the weak Z current (see, e.g., Ref. [52]), which appears at $\mathcal{O}(m_{A'}^2/m_Z^2)$. We provide nearly model-independent sensitivity estimates for the mass range $m_{A'} \lesssim 10$ GeV by ignoring the coupling to the Z. We include model-dependent Z-mixing effects for $m_{A'} \gtrsim 10$ GeV, adopting the parameters of Refs. [53,54].

The partial widths of A' to SM leptons are

$$\Gamma_{A' \to \ell^+\ell^-} = \frac{\epsilon^2 \alpha_{EM}}{3} m_{A'} \left(1 + 2\frac{m_\ell^2}{m_{A'}^2}\right)\sqrt{1 - 4\frac{m_\ell^2}{m_{A'}^2}}, \tag{3}$$

where $\ell = e, \mu, \tau$ and $m_{A'} > 2m_\ell$. Because the A' couples to J_{EM}^μ, the branching fraction of A' to SM hadrons can be extracted from the measured value of $\mathcal{R}_\mu \equiv \sigma_{e^+e^- \to hadrons}/\sigma_{e^+e^- \to \mu^+\mu^-}$ (taken from Ref. [55]):

$$\Gamma_{A' \to hadrons} = \Gamma_{A' \to \mu^+\mu^-}\mathcal{R}_\mu(m_{A'}^2). \tag{4}$$

In particular, Eq. (4) already includes the effect of the A' mixing with the QCD vector mesons ρ, ω, ϕ, etc. It is also possible for the A' to couple to non-SM particles with an invisible decay width $\Gamma_{A' \to invisible}$, in which case the total A' width is

$$\Gamma_{A'} = \sum_\ell \Gamma_{A' \to \ell^+\ell^-} + \Gamma_{A' \to hadrons} + \Gamma_{A' \to invisible}. \tag{5}$$
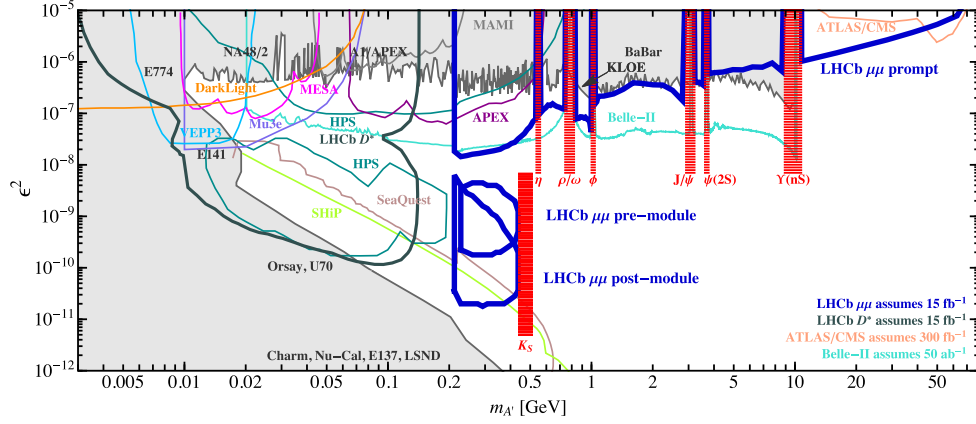
FIG. 1. Previous and planned experimental bounds on dark photons (adapted from [1]) compared to the anticipated LHCb reach for inclusive A' production in the dimuon channel (see the text for definitions of prompt, pre-module, and post-module). The red vertical bands indicate QCD resonances which would have to be masked in a complete analysis. The LHCb D^* anticipated limit comes from [48], and Belle-II comes from [49].

Below, we consider $\Gamma_{A' \to \text{invisible}} = 0$, though our analysis can be easily adapted to handle nonvanishing invisible decay modes.

To estimate the $A' \to \mu^+ \mu^-$ signal rate, we follow the strategy outlined in Ref. [7]. Consider the signal production process in proton-proton (pp) collisions

$$S: pp \to XA' \to X\mu^+\mu^-, \qquad (6)$$

where X is any (multiparticle) final state. Ignoring $\mathcal{O}(m_{A'}^2/m_Z^2)$ and $\mathcal{O}(\alpha_{\text{EM}})$ corrections, this process has the identical cross section to the prompt SM process which originates from the EM current

$$B_{\text{EM}}: pp \to X\gamma^* \to X\mu^+\mu^-, \qquad (7)$$

up to differences between the A' and γ^* propagators and the kinetic-mixing suppression. Interference between S and B_{EM} is negligible for a narrow A' resonance. Therefore, for *any* selection criteria on X, μ^+, and μ^-, the ratio between the differential cross sections is

$$\frac{d\sigma_{pp \to XA' \to X\mu^+\mu^-}}{d\sigma_{pp \to X\gamma^* \to X\mu^+\mu^-}} = \epsilon^4 \frac{m_{\mu\mu}^4}{(m_{\mu\mu}^2 - m_{A'}^2)^2 + \Gamma_{A'}^2 m_{A'}^2}, \qquad (8)$$

where $m_{\mu\mu}$ is the dimuon invariant mass, for the case $\Gamma_{A'} \ll |m_{\mu\mu} - m_{A'}| \ll m_{A'}$. The ϵ^4 factor arises because both the A' production and decay rates scale like ϵ^2.

To obtain a signal event count, we integrate over an invariant-mass range of $|m_{\mu\mu} - m_{A'}| < 2\sigma_{m_{\mu\mu}}$, where $\sigma_{m_{\mu\mu}}$ is the detector resolution on $m_{\mu\mu}$. The ratio of signal events to prompt EM background events is

$$\frac{S}{B_{\text{EM}}} \approx \epsilon^4 \frac{\pi}{8} \frac{m_{A'}^2}{\Gamma_{A'} \sigma_{m_{\mu\mu}}} \approx \frac{3\pi}{8} \frac{m_{A'}}{\sigma_{m_{\mu\mu}}} \frac{\epsilon^2}{\alpha_{\text{EM}}(N_\ell + \mathcal{R}_\mu)}, \qquad (9)$$

neglecting phase space factors for N_ℓ leptons lighter than $m_{A'}/2$. This expression already accounts for the $A' \to \mu^+\mu^-$ branching-fraction suppression when $\mathcal{R}_\mu$ is large. Despite

the factor of ϵ^4 in Eq. (8), the ratio in Eq. (9) is proportional to ϵ^2 because of the ϵ^2 scaling of $\Gamma_{A'}$.

We emphasize that Eq. (9) holds for *any* final state X (and any kinematic selection) in the $m_{A'} \ll m_Z$ limit for tree-level single-photon processes. In particular, it already includes $\mu^+\mu^-$ production from QCD vector mesons that mix with the photon. This allows us to perform a fully data-driven analysis, since the efficiency and acceptance for the (measured) prompt SM process is the same as for the (inferred) signal process, excluding A' lifetime-based effects. The dominant component of B_{EM} at small $m_{A'}$ comes from meson decays $M \to \mu^+\mu^- Y$, especially $\eta \to \mu^+\mu^-\gamma$, and is denoted as B_M (which includes feed-down contributions from heavier meson decays). There are also two other important components: final state radiation (FSR) and Drell-Yan (DY) production. Nonprompt γ^* production is small and only considered as a background.

Beyond B_{EM}, there are other important sources of backgrounds that contribute to the reconstructed prompt dimuon sample, ordered by their relative size: $B_{\text{misID}}^{\pi\pi}$—Two pions (and more rarely a kaon and pion) can be misidentified (misID) as a fake dimuon pair, including the contribution from in-flight decays. This background can be deduced and subtracted in a data-driven way using prompt same-sign dimuon candidates [56,57]. $B_{\text{misID}}^{\pi\mu}$—A fake dimuon pair can also arise from one real muon (primarily from charm or beauty decays) combined with one misID pion or kaon. This background can be subtracted similarly to $B_{\text{misID}}^{\pi\pi}$. B_{BH}—The Bethe-Heitler (BH) background played an important role in the analysis of Ref. [7]. This is a subdominant process at the LHC due in part to the small effective photon luminosity function. We verified that B_{BH} is small using a parton shower generator (see below), and it will be neglected in estimating the reach. True displaced dimuon pairs, which arise from beauty decays, are rarely reconstructed as

prompt at LHCb. Such backgrounds, however, are dominant in the displaced search discussed below.

Summarizing, the reconstructed prompt dimuon sample contains the following background components:

$$B_{\text{prompt}} = \underbrace{B_M + B_{\text{FSR}} + B_{\text{DY}}}_{B_{\text{EM}}} + \underbrace{B_{\text{misID}}^{\pi\pi} + B_{\text{misID}}^{\pi\mu}}_{B_{\text{misID}}}, \quad (10)$$

where for simplicity we ignore interference terms between the various B_{EM} components. After subtracting B_{misID} from B_{prompt} [56,57], we can use Eq. (9) to infer S from B_{EM} for any $m_{A'}$ and ϵ^2. Since both B_{prompt} and B_{misID} are extracted from data, this strategy is fully data driven.

We now present an inclusive search strategy for dark photons at the LHCb. The LHCb experiment will upgrade to a triggerless detector-readout system for run 3 of the LHC [62], making it highly efficient at selecting $A' \to \mu^+\mu^-$ decays in real time. Therefore, we focus on run 3 and assume an integrated luminosity of (see Ref. [48])

$$\int \mathcal{L}dt = 15 \text{ fb}^{-1}. \quad (11)$$

The trigger system currently employed by LHCb is efficient for many $A' \to \mu^+\mu^-$ decays included in our search. We estimate that the sensitivity in run 2 will be equivalent to using about 10% of the data collected in run 3. Therefore, inclusion of run 2 data will not greatly impact the reach by the end of run 3, though a run 2 analysis could explore much of the same $m_{A'} - \epsilon^2$ parameter space in the next few years.

The LHCb detector is a forward spectrometer covering the pseudorapidity range $2 < \eta < 5$ [63,64]. Within this acceptance, muons with three-momentum $p > 5$ GeV are reconstructed with near 100% efficiency with a momentum resolution of $\sigma_p/p \approx 0.5\%$ and a dimuon invariant mass resolution of [64,65]

$$\sigma_{m_{\mu\mu}} \approx \begin{cases} 4 \text{ MeV} & m_{\mu\mu} < 1 \text{ GeV} \\ 0.4\%m_{\mu\mu} & m_{\mu\mu} > 1 \text{ GeV} \end{cases}. \quad (12)$$

For the displaced A' search, the vertex resolution of LHCb depends on the Lorentz boost factor of the A'; we therefore use an event-by-event selection criteria in the analysis below. That said, it is a reasonable approximation to use a fixed A' proper-lifetime resolution [64]

$$\sigma_\tau \approx 50 \text{ fs}, \quad (13)$$

except near the dimuon threshold where the opening angle between the muons is small.

To suppress fake muons, our strategy requires muon candidates have (transverse) momenta ($p_T > 0.5$ GeV) $p > 10$ GeV, and are selected by a neural-network muon-identification algorithm [58] with a muon efficiency of $\epsilon_\mu^2 \approx 0.50$ and a pion fake rate of $\epsilon_\pi^2 \approx 10^{-6}$ [57]. To a good approximation, the neural-network performance is independent of the kinematics. Such a low pion misID rate

is a unique feature of LHCb and is vital for probing the low-$m_{A'}$ region in $A' \to \mu^+\mu^-$ decays.

To further suppress B_{misID} for $m_{A'} > m_\phi \simeq 1.0$ GeV, we require muons to satisfy an isolation criterion based on clustering the charged component of the final state with the anti-k_T jet algorithm [66] with $R = 0.5$ in FASTJET 3.1.2 [67]; muons with $p_T(\mu)/p_T(\text{jet}) < 0.85$ are rejected, excluding the contribution to $p_T(\text{jet})$ from the other muon if it is contained in the same jet. By considering charged particles only, this isolation strategy is robust to pileup. The dimuon isolation efficiencies obtained from simulated LHCb data (see below) are 50% for FSR, DY, and BH, 25% for meson decays (dominantly from charmonium states), and 1% for fake pions ($\pi\pi$ and $\pi\mu$ have similar efficiencies).

The baseline selection for the LHCb inclusive A' search is, therefore, (i) two opposite-sign muons with $\eta(\mu^\pm) \in [2, 5]$, $p(\mu^\pm) > 10$ GeV, and $p_T(\mu^\pm) > 0.5$ GeV; (ii) a reconstructed $A' \to \mu^+\mu^-$ candidate with $\eta(A') \in [2, 5]$, $p_T(A') > 1$ GeV, and passing the isolation criterion for $m_{A'} > m_\phi$; (iii) an $A' \to \mu^+\mu^-$ decay topology consistent with either a prompt or displaced A' decay [48,57].

Following a similar strategy to Ref. [48], we use the reconstructed muon impact parameter (IP) and A' transverse flight distance ℓ_T to define three nonoverlapping search regions: (i) Prompt.—$\text{IP}_{\mu^\pm} < 2.5\sigma_{\text{IP}}$; (ii) Displaced (premodule).—$\ell_T \in [5\sigma_{\ell_T}, 6 \text{ mm}]$; (iii) Displaced (postmodule).—$\ell_T \in [6 \text{ mm}, 22 \text{ mm}]$.

The resolution on IP and ℓ_T are taken from Refs. [57,59]. The displaced A' search is restricted to $\ell_T < 22$ mm to ensure at least three hits per track in the vertex locator (VELO). We define two search regions based on the average ℓ_T to the first VELO module (i.e., 6 mm), where each VELO module is a planar silicon-pixel detector oriented perpendicular to the LHC beam line.

To estimate the reach for this A' search using the data-driven strategy in Eq. (9), we need to know $B_{\text{prompt}}(m_{\mu\mu})$ with the above selection criteria applied. To our knowledge, LHCb has not published such a spectrum, so we use PYTHIA 8.212 [68] for illustrative purposes to understand the various components of B_{EM}. (We caution the reader that the dimuon spectra published by ATLAS [69] and CMS [70] do not impose prompt selection criteria nor do they subtract fake dimuons). LHCb has published measurements of ϕ meson [71], charmonium [72], bottomonium [73], and DY [74] production in 7 TeV pp collisions, and we find that PYTHIA accurately reproduces these measurements. Therefore, we assume that PYTHIA also adequately predicts their production at 14 TeV. The ALICE Collaboration has published the low-mass dimuon spectrum at $\sqrt{s} = 7$ TeV in a similar kinematic region as proposed for this search [56]. Within the kinematic region used by ALICE, we find that PYTHIA accurately describes the production of the $\eta^{(\prime)}$ mesons, but overestimates ω and ρ production by factor of 2; we therefore reduce the

PYTHIA prediction for these mesons to match the observed ALICE spectrum.

Including our selection criteria and modifications, the prompt dimuon spectrum from PYTHIA is shown in Fig. 2. The B_{EM} background is dominated by meson decays like $\eta \to \mu^+ \mu^- \gamma$ at low invariant mass, and transitions to DY production $pp \to \gamma^* \to \mu^+ \mu^-$ at larger $m_{\mu\mu}$, with FSR being subdominant throughout. Note the sharp change in the spectrum at $m_{\mu\mu} = m_\phi$ due to the muon-isolation requirement. We also show in Fig. 2 the expected non-EM background contamination from B_{misID} and B_{BH}. The misidentification background is large and dominates for $m_{A'} \in [1, 3]$ GeV, though this is also the region where PYTHIA likely underestimates dimuon production from excited meson decays [e.g., $\rho(1450) \to \mu^+ \mu^-$] [57].

We also use PYTHIA to understand the backgrounds for the displaced A' searches, where the dominant contribution comes from double semileptonic heavy-flavor decays of the form $b \to c\mu^\pm X$ followed by $c \to \mu^\mp Y$. Such decays are highly suppressed by our consistent-decay-topology requirements [57], but they still contribute at a large rate because of the copious heavy-flavor production in high-energy pp collisions. Semileptonic decays of charm and beauty mesons, where one real muon and one fake muon arise from the same secondary vertex, also contribute but at a much lower rate. Decays of heavy-flavor hadrons with two misID pions or with $\gamma^* \to \mu^+ \mu^-$ are similarly subdominant.

For the premodule displaced region, we find $\approx 10^4$ background events per $\pm 2\sigma_{m_{\mu\mu}}$ mass bin. For the post-module displaced region, relevant for long-lived dark photons with $\tau_{A'} \gg \tau_{D,B}$, we estimate the background to be ≈ 25 candidates per mass bin by scaling the observed combinatorial background in a published LHCb $K_S \to \mu^+ \mu^-$ search [58] by the increase in luminosity used in this analysis. In the postmodule region, the heavy-flavor background is on the order of few events per bin, and the dominant contribution is from interactions with the detector
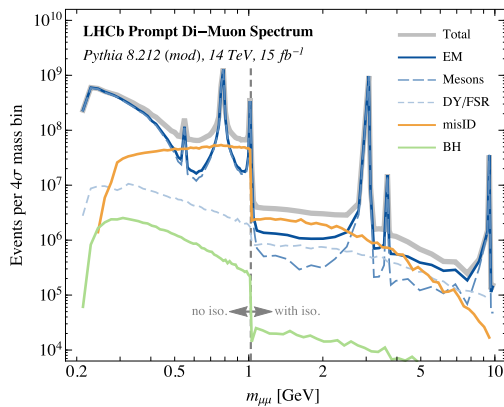

FIG. 2. Predicted reconstructed dimuon invariant mass spectrum with our prompt selection criteria applied after run 3, including the isolation criteria for $m_{\mu\mu} > m_\phi$. "EM" denotes the sum of "Mesons" and "DY/FSR".

material. This contribution can likely be reduced following a strategy similar to [48].

The estimated sensitivity of LHCb to inclusive A' production is shown in Fig. 1. For the prompt A' search, we estimate S from B_{EM} using data in the neighboring sidebands and take $S/\sqrt{B_{prompt}} \approx 2$ as a rough criterion for the exclusion limit. This sideband method fails near narrow QCD resonances, which would need a dedicated analysis. Figure 1 shows that for $m_{A'} \in [2m_\mu, m_\phi]$ one can probe ϵ^2 down to 10^{-8}–10^{-7} with the prompt search, improving on current limits. The reach is limited at higher masses due to B_{misID}, where the expected sensitivity is comparable to the present bound. Going to higher masses where the A' production rate depends on model-dependent mixing with the Z, LHCb can extend anticipated ATLAS and CMS limits [45] for $m_{A'} \in [10, 40]$ GeV.

For the displaced A' search, the spectrum of A' Lorentz boost factors $\gamma_{\mu\mu} \equiv E_{\mu\mu}/m_{\mu\mu}$ can be inferred from the prompt $\gamma^* \to \ell^+ \ell^-$ spectrum observed in data in a given $m_{\mu\mu}$ bin; the A' lifetime acceptance can then be obtained from simulation. Following the background discussion above, the exclusion criterion for the premodule (post-module) search is $S \approx 2\sqrt{B} \approx 200$ ($S \approx 2\sqrt{B} \approx 10$), yielding the regions shown in Fig. 1. A comparable reach is obtained by simply assuming the fixed proper-lifetime resolution in Eq. (13). Because of the large $\eta \to \gamma A'$ rate, the displaced search has the potential to probe $m_{A'} \in [2m_\mu, m_\eta]$ with $\epsilon \in [10^{-11}, 10^{-8}]$, a region that is challenging to access through other experiments.

There are a number of possible improvements and generalizations to this A' search. For example, dark photons can be searched for during LHC run 2, by adapting our analysis to include dimuon hardware trigger requirements. Because the search is entirely data driven, dimuon triggers need not be fully efficient to be useful in such an analysis. The real-time analysis, event selection, and multi-search-region [60] strategies employed by LHCb could be improved, and data collected in LHC runs 4 and 5 would greatly improve the sensitivity [57]. One could also pursue a semi-inclusive strategy, where an A' candidate is selected along with another required object; for most semi-inclusive modes, one can still use the data-driven method in Eq. (9). If the fake muon backgrounds could be controlled, a similar search could be performed at ATLAS and CMS. Beyond dark photons, these searches are sensitive to spin-0 dimuon resonances (see related work in Refs. [75–77]). An inclusive A' search in the electron channel could explore the $m_{A'} \in [2m_e, 2m_\mu]$ mass region, though this is considerably more challenging due to bremsstrahlung radiation and multiple scattering [57].

In summary, we proposed an inclusive search strategy for dark photons at the LHCb experiment using dimuon resonances. Since the coupling of the A' to the standard model is dictated by the kinetic-mixing parameter ϵ^2, the signal rate can be directly inferred from the off-shell photon rate,

enabling a data-driven search. Through a combination of prompt and displaced searches, LHCb is sensitive to interesting regions in the $m_{A'} - \epsilon^2$ parameter space, some of which are difficult to probe with other proposed experiments. This search leverages the excellent invariant-mass and vertex resolution of LHCb, along with its unique particle-identification and real-time data-analysis capabilities. Provided that the appropriate real-time selections are employed starting this year, LHCb could probe much of this parameter space using data collected in run 2 of the LHC. Given the simplicity of this proposed search strategy, it could easily be adapted to other experiments at the LHC and beyond.

---

*philten@cern.ch
†soreqy@mit.edu
‡jthaler@mit.edu
§mwill@mit.edu
‖weixue@mit.edu

[1] R. Essig *et al.*, arXiv:1311.0029.
[2] L. B. Okun, Zh. Eksp. Teor. Fiz. **83**, 892 (1982) [JETP **56**, 502 (1982)].
[3] P. Galison and A. Manohar, Phys. Lett. **136B**, 279 (1984).
[4] B. Holdom, Phys. Lett. **166B**, 196 (1986).
[5] M. Pospelov, A. Ritz, and M. B. Voloshin, Phys. Lett. B **662**, 53 (2008).
[6] N. Arkani-Hamed, D. P. Finkbeiner, T. R. Slatyer, and N. Weiner, Phys. Rev. D **79**, 015014 (2009).
[7] J. D. Bjorken, R. Essig, P. Schuster, and N. Toro, Phys. Rev. D **80**, 075018 (2009).
[8] F. Bergsma *et al.* (CHARM Collaboration), Phys. Lett. **166B**, 473 (1986).
[9] A. Konaka *et al.*, Phys. Rev. Lett. **57**, 659 (1986).
[10] E. M. Riordan *et al.*, Phys. Rev. Lett. **59**, 755 (1987).
[11] J. D. Bjorken, S. Ecklund, W. R. Nelson, A. Abashian, C. Church, B. Lu, L. W. Mo, T. A. Nunamaker, and P. Rassmann, Phys. Rev. D **38**, 3375 (1988).
[12] A. Bross, M. Crisler, S. H. Pordes, J. Volk, S. Errede, and J. Wrbanek, Phys. Rev. Lett. **67**, 2942 (1991).
[13] M. Davier and H. Nguyen Ngoc, Phys. Lett. B **229**, 150 (1989).
[14] C. Athanassopoulos *et al.* (LSND Collaboration), Phys. Rev. C **58**, 2489 (1998).
[15] P. Astier *et al.* (NOMAD Collaboration), Phys. Lett. B **506**, 27 (2001).
[16] S. Adler *et al.* (E787 Collaboration), Phys. Rev. D **70**, 037102 (2004).
[17] A. V. Artamonov *et al.* (BNL-E949 Collaboration), Phys. Rev. D **79**, 092004 (2009).
[18] R. Essig, R. Harnik, J. Kaplan, and N. Toro, Phys. Rev. D **82**, 113008 (2010).
[19] J. Blumlein and J. Brunner, Phys. Lett. B **701**, 155 (2011).
[20] S. Gninenko, Phys. Lett. B **713**, 244 (2012).
[21] J. Blumlein and J. Brunner, Phys. Lett. B **731**, 320 (2014).
[22] S. Abrahamyan *et al.* (APEX Collaboration), Phys. Rev. Lett. **107**, 191804 (2011).
[23] H. Merkel *et al.*, Phys. Rev. Lett. **112**, 221802 (2014).
[24] H. Merkel *et al.* (A1 Collaboration), Phys. Rev. Lett. **106**, 251802 (2011).
[25] B. Aubert *et al.* (*BABAR* Collaboration), Phys. Rev. Lett. **103**, 081803 (2009).
[26] D. Curtin *et al.*, Phys. Rev. D **90**, 075004 (2014).
[27] J. P. Lees *et al.* (*BABAR* Collaboration), Phys. Rev. Lett. **113**, 201801 (2014).
[28] G. Bernardi, G. Carugno, J. Chauveau, F. Dicarlo, M. Dris *et al.*, Phys. Lett. **166B**, 479 (1986).
[29] R. Meijer Drees *et al.* (SINDRUM I Collaboration), Phys. Rev. Lett. **68**, 3845 (1992).
[30] F. Archilli *et al.* (KLOE-2 Collaboration), Phys. Lett. B **706**, 251 (2012).
[31] S. N. Gninenko, Phys. Rev. D **85**, 055027 (2012).
[32] D. Babusci *et al.* (KLOE-2 Collaboration), Phys. Lett. B **720**, 111 (2013).
[33] P. Adlarson *et al.* (WASA-at-COSY Collaboration), Phys. Lett. B **726**, 187 (2013).
[34] G. Agakishiev *et al.* (HADES Collaboration), Phys. Lett. B **731**, 265 (2014).
[35] A. Adare *et al.* (PHENIX Collaboration), Phys. Rev. C **91**, 031901 (2015).
[36] J. R. Batley *et al.* (NA48/2 Collaboration), Phys. Lett. B **746**, 178 (2015).
[37] A. Anastasi *et al.* (KLOE-2 Collaboration), Phys. Lett. B **757**, 356 (2016).
[38] R. Essig, P. Schuster, N. Toro, and B. Wojtsekhowski, J. High Energy Phys. 02 (2011) 009.
[39] M. Freytsis, G. Ovanesyan, and J. Thaler, J. High Energy Phys. 01 (2010) 111.
[40] J. Balewski, J. Bernauer, W. Bertozzi, J. Bessuille, B. Buck *et al.*, arXiv:1307.4432.
[41] B. Wojtsekhowski, D. Nikolenko, and I. Rachek, arXiv:1207.5089.
[42] T. Beranek, H. Merkel, and M. Vanderhaeghen, Phys. Rev. D **88**, 015032 (2013).
[43] B. Echenard, R. Essig, and Y.-M. Zhong, J. High Energy Phys. 01 (2015) 113.
[44] M. Battaglieri *et al.*, Nucl. Instrum. Methods Phys. Res., Sect. A **777**, 91 (2015).
[45] D. Curtin, R. Essig, S. Gori, and J. Shelton, J. High Energy Phys. 02 (2015) 157.
[46] S. Alekhin *et al.*, arXiv:1504.04855.
[47] S. Gardner, R. J. Holt, and A. S. Tadepalli, Phys. Rev. D **93**, 115015 (2016).
[48] P. Ilten, J. Thaler, M. Williams, and W. Xue, Phys. Rev. D **92**, 115017 (2015).

[49] C. Hearty (private communication).

[50] S. Benson, V. Gligorov, M. A. Vesterinen, and M. Williams, J. Phys. Conf. Ser. **664**, 082004 (2015).

[51] R. Aaij *et al.* (LHCb Collaboration), J. High Energy Phys. 03 (2016) 159.

[52] G. Barello, S. Chang, and C. A. Newby, arXiv:1511.02865.

[53] S. Cassel, D. M. Ghilencea, and G. G. Ross, Nucl. Phys. **B827**, 256 (2010).

[54] J. M. Cline, G. Dupuis, Z. Liu, and W. Xue, J. High Energy Phys. 08 (2014) 131.

[55] K. A. Olive *et al.* (Particle Data Group Collaboration), Chin. Phys. C **38**, 090001 (2014).

[56] B. Abelev *et al.* (ALICE Collaboration), Phys. Lett. B **710**, 557 (2012).

[57] See Supplemental Material at http://link.aps.org/supplemental/10.1103/PhysRevLett.116.251803 for a more detailed discussion of the misID background, muon performance, consistent-decay-topology requirements, and possible improvements, which includes Refs. [48,58–61].

[58] R. Aaij *et al.* (LHCb Collaboration), J. High Energy Phys. 02 (2015) 121.

[59] R. Aaij *et al.* (LHCb Collaboration), LHCb VELO Upgrade Technical Design Report No. LHCb-TDR-013, 2013.

[60] M. Williams, J. Instrum. **10**, P06002 (2015).

[61] M. Adinolfi *et al.*, Eur. Phys. J. C **73**, 2431 (2013).

[62] R. Aaij *et al.* (LHCb Collaboration),LHCb Trigger and Online Technical Design Report No. LHCb-TDR-016, 2014.

[63] A. A. Alves, Jr.*et al.* (LHCb Collaboration), J. Instrum. **3**, S08005 (2008).

[64] R. Aaij *et al.* (LHCb Collaboration), Int. J. Mod. Phys. A **30**, 1530022 (2015).

[65] R. Aaij *et al.* (LHCb Collaboration), J. High Energy Phys. 01 (2013) 090.

[66] M. Cacciari, G. P. Salam, and G. Soyez, J. High Energy Phys. 04 (2008) 063.

[67] M. Cacciari, G. P. Salam, and G. Soyez, Eur. Phys. J. C **72**, 1896 (2012).

[68] T. Sjstrand, S. Ask, J. R. Christiansen, R. Corke, N. Desai, P. Ilten, S. Mrenna, S. Prestel, C. O. Rasmussen, and P. Z. Skands, Comput. Phys. Commun. **191**, 159 (2015).

[69] G. Aad *et al.* (ATLAS Collaboration), Eur. Phys. J. C **74**, 3034 (2014).

[70] S. Chatrchyan *et al.* (CMS Collaboration), J. Instrum. **7**, P10002 (2012).

[71] R. Aaij *et al.* (LHCb Collaboration), Phys. Lett. B **703**, 267 (2011).

[72] R. Aaij *et al.* (LHCb Collaboration), Eur. Phys. J. C **71**, 1645 (2011).

[73] R. Aaij *et al.* (LHCb Collaboration), Eur. Phys. J. C **72**, 2025 (2012).

[74] R. Aaij *et al.* (LHCb Collaboration), LHCb, LHCb-CONF-2012-013, CERN-LHCb-CONF-2012-013, 2012.

[75] M. Freytsis, Z. Ligeti, and J. Thaler, Phys. Rev. D **81**, 034001 (2010).

[76] R. Aaij *et al.* (LHCb Collaboration), Phys. Rev. Lett. **115**, 161802 (2015).

[77] U. Haisch and J. F. Kamenik, Phys. Rev. D **93**, 055047 (2016).